

ELECTRONIC SUPPLEMENTARY INFORMATION (ESI)

Structurally diverse zinc(II) complexes containing tripodal tetradentate phenoxido-amines with promising antiproliferative effects[†]

Salah S. Massoud,^{*a,b} Franz A. Mautner,^{*c} Febee R. Louka,^a Nahed M. H. Salem,^b Roland C. Fischer,^d Ana Torvisco,^d Ján Vančo,^e Jan Belza,^e Zdeněk Dvořák^f and Zdeněk Trávníček^{*,e}

The authors would like to dedicate this work to Jan Belza, our beloved colleague and friend, who passed away unexpectedly at the age of 31 years.

- ^a Department of Chemistry, University of Louisiana at Lafayette, P.O. Box 43700, Lafayette, LA 70504, U.S.A.
- ^b Department of Chemistry, Faculty of Science, Alexandria University, Moharam Bey 21511, Alexandria, Egypt
- ^c Institut für Physikalische and Theoretische Chemie, Technische Universität Graz, Stremayrgasse 9/II, A-8010, Graz, Austria
- ^d Institut für Anorganische Chemische, Technische Universität Graz, Stremayrgasse 9/V, A-8010 Graz, Austria
- ^e Czech Advanced Technology and Research Institute, Regional Centre of Advanced Technologies and Materials, Palacký University, Šlechtitelů 27, CZ-779 00 Olomouc, Czech Republic
- ^f Department of Cell Biology and Genetics, Faculty of Science, Palacký University, Šlechtitelů 27, CZ-783 71 Olomouc, Czech Republic

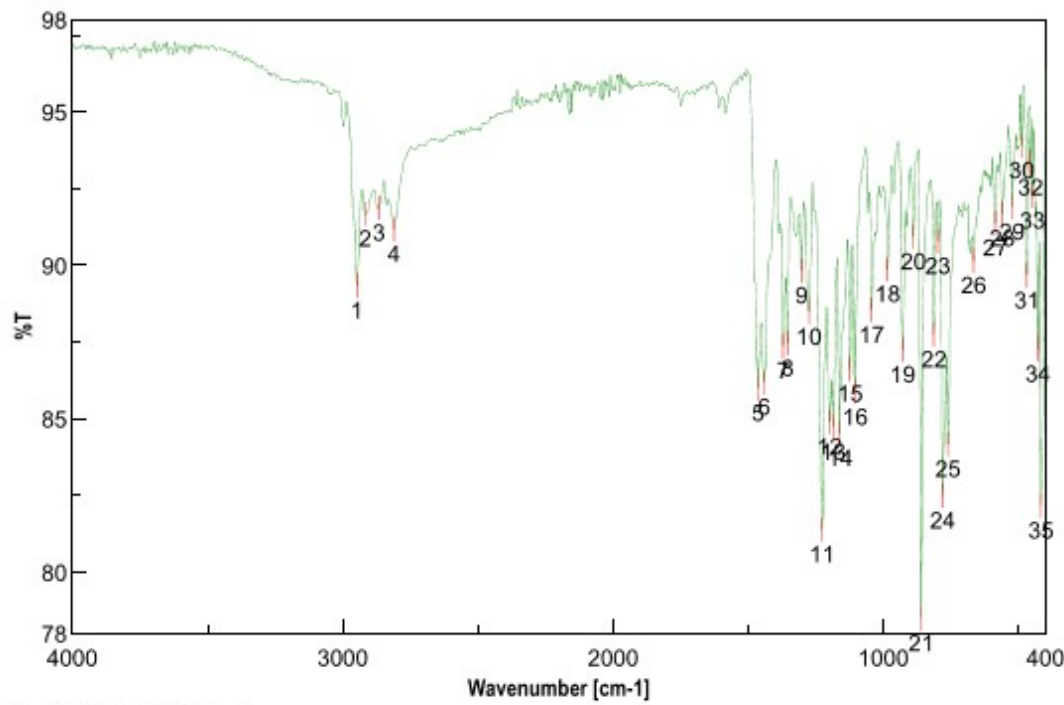
Contents	page #
Synthesis of H_2L^3	2
Fig. S1. IR spectrum of H_2L^3	4
Fig. S2. ^1H NMR spectra of H_2L^3 in d_6 -DMSO.....	5
Fig. S3. ESI-MS of H_2L^3 in CH_3OH	6
Fig. S4. IR spectrum of $[\text{Zn}_2(\text{L}^1)_2](\text{ClO}_4)_2$ 1	7
Fig. S5. IR spectrum of $[\text{Zn}_2(\text{L}^2)_2](\text{ClO}_4)_2$ 2	8
Fig. S6. IR spectrum of $[\text{Zn}(\text{L}^3)(\text{H}_2\text{O})]\cdot\text{CH}_3\text{OH}$ 3	9
Fig. S7. IR spectrum of 4	10
Fig. S8. IR spectrum of 5	11
Fig. S9. IR spectrum of 6	12
Fig. S10. ESI-MS of H_2L^4 in CH_3OH	13
Fig. S11. ESI-MS of complex 3 in CH_3CN	13
Fig. S12. ESI-MS of complex 4 in CH_3CN	14
Fig. S13. ESI-MS of complex 5 in CH_3CN	14

Fig. S14. ESI-MS of complex 6 in CH ₃ CN	15
Fig. S15. ESI-MS of complex 1 in CH ₃ CN	15
Fig. S16. ESI-MS of complex 2 in CH ₃ CN/HCOOH (1:1) mixture	16
Fig. S17. UV spectrum of 1 in MeOH	16
Fig. S18. UV spectrum of 2 in CH ₃ CN (top) and in DMSO (bottom)	17
Fig. S19. UV spectrum of 4 in CH ₃ CN	18
Fig. S20: ORTEP view of complex 1 showing disordered parts of the complex.	18
Fig. S21. Packing plot of 1	19
Fig. S22. Packing plot of 2	19
Fig. S23. Packing plot of 3	20
Fig. S24. Packing plot of 4	20
Fig. S25. Packing plot of 5	21
Fig. S26. Packing plot of 6	21
Fig. S27. ¹ H NMR spectrum of free H ₂ L ⁴ measured in CDCl ₃	22
Fig. S28. ¹³ C NMR spectrum of free H ₂ L ⁴ measured in CDCl ₃	22
Fig. S29. ¹ H NMR spectrum of [Zn(L ⁴)] (4) measured in CDCl ₃ immediately after the sample dissolution.	23
Fig. S30. ¹ H NMR spectrum of [Zn(L ⁴)] (4) measured in CDCl ₃ 22 h after the sample dissolution.	23
Fig. S31. ¹ H NMR spectrum of [Zn(L ⁴)] (4) measured in CDCl ₃ 6 days after the sample dissolution.	24
Fig. S32. ¹³ C NMR spectrum of [Zn(L ⁴)] (4) measured in CDCl ₃ immediately after the sample dissolution.	24
Fig. S33. ¹³ C NMR spectrum of [Zn(L ⁴)] (4) measured in CDCl ₃ 22 h after the sample dissolution. *The selected signals belonging to the free H ₂ L ⁴ ligand.	25
Fig. S34. ¹³ C NMR spectrum of [Zn(L ⁴)] (4) measured in CDCl ₃ 6 days after the sample dissolution. *The selected signals belonging to the free H ₂ L ⁴ ligand.	25
Fig. S35. The effect of complexes 2 , 3 and 5 , and ligand H ₂ L ⁶ on intracellular levels of zinc in A2780 cells	26

Synthesis of 6,6'-(((2-(Dimethylamino)ethyl)azanediyl)bis(methylene))bis(2-(*tert*-butyl)-4-methylphenol), H₂L³. A mixture of 2-*tert*-butyl-4-methylphenol (8.213 g, 50 mmol), Et₃N (5.052 g, 50 mmol), 37% HCHO (4.173 g, 50 mmol) and *N,N*-dimethylethylenediamine (2.204 g, 25 mmol) was dissolved in methanol (60 mL). The reaction mixture was stirred under gentle reflux for 3 days, then the solution was reduced to half of its volume by a rotary evaporator. The white precipitate, which was obtained was collected by filtration, recrystallized from EtOAc, washed with Et₂O, and air dried (yield: 4.85 g, 47.7 %). Characterization: Anal. Calcd for C₂₈H₄₄N₂O₂ (MM = 441.3489 g/mol): C, 76.32; H, 10.06; N, 6.36%. Found: C, 76.50; H, 10.24; N, 6.35%. m.p. 167-170° C. ESI-MS (MeOH): *m/z* = 469.3804 (100%), Calcd [H₂L³+H]⁺ = 441.34812. IR bands (ATR, cm⁻¹): ~3200 (sh) ν(O-H); 2947 (m), 2917 (vw), 2867 (vw), 2810 (w)

ν (C-H); 1570 (vw) ν (C=N); 1465 (s), 1442 (s), 1371 (s), 1354 (s) ν (C=C, C-N, C-O); 1226 (vs), 1200(s), 1186 (s), 1123 (m), 1105 (m), 1043 (m), 984 (m), 762 (s), 470 (m), 429 (m), 418 (vs). ^1H NMR (d_6 -DMSO, 400 MHz, δ in ppm): δ = 6.89, 6.76 (s, 1H each, protons-ph); 3.51, 3.17 (s, 2H, N- $\underline{\text{CH}_2}$ -ph); 2.20, 2.17 (s, 3H, CH_3 -N; 8H, N- CH_2 - CH_2 -N); CH_3 -ph); 1.32 (s, 9H, $(\text{CH}_3)_3\text{C}$).

Peak Find - 3830.jws



[Result of Peak Picking]

No.	Position	Intensity	No.	Position	Intensity
1	2946.7	89	2	2916.81	92
3	2866.67	92	4	2809.78	91
5	1464.67	86	6	1441.53	86
7	1371.14	87	8	1354.75	87
9	1302.68	90	10	1274.72	88
11	1226.5	81	12	1199.51	85
13	1186.01	85	14	1160.94	85
15	1123.33	87	16	1105.01	86
17	1043.3	89	18	984.482	90
19	928.557	87	20	889.987	91
21	860.096	78	22	813.813	88
23	798.385	91	24	781.029	82
25	761.744	84	26	666.285	90
27	586.254	91	28	561.184	92
29	524.543	92	30	488.866	94
31	469.582	90	32	456.082	93
33	448.369	92	34	429.084	87
35	417.513	82			

Fig. S1. IR spectrum of H₂L³.

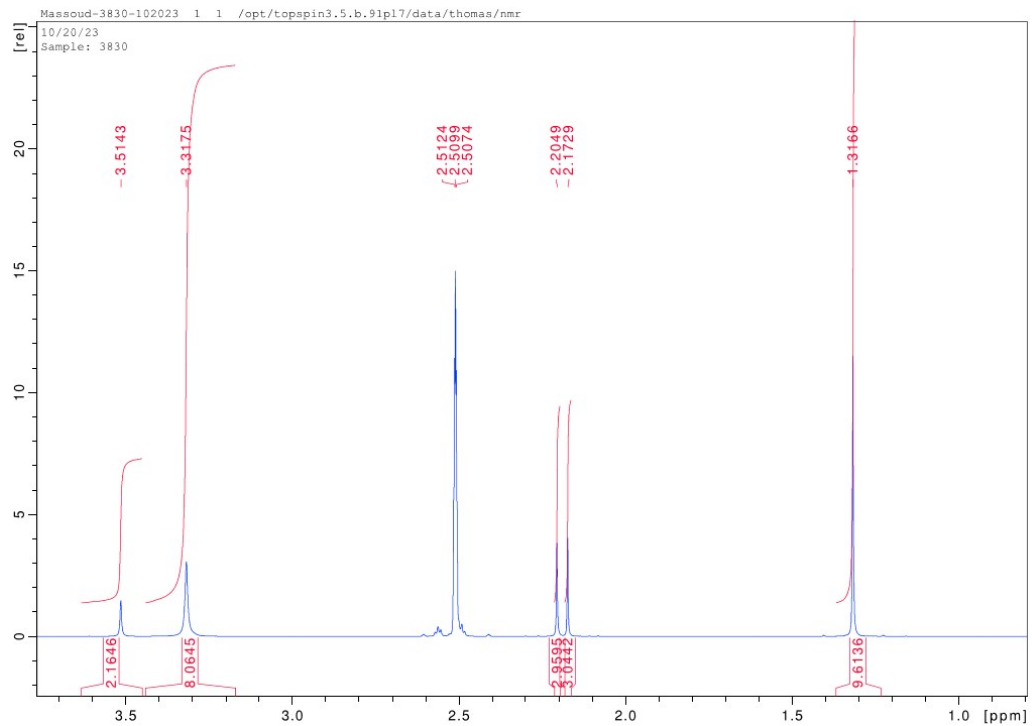
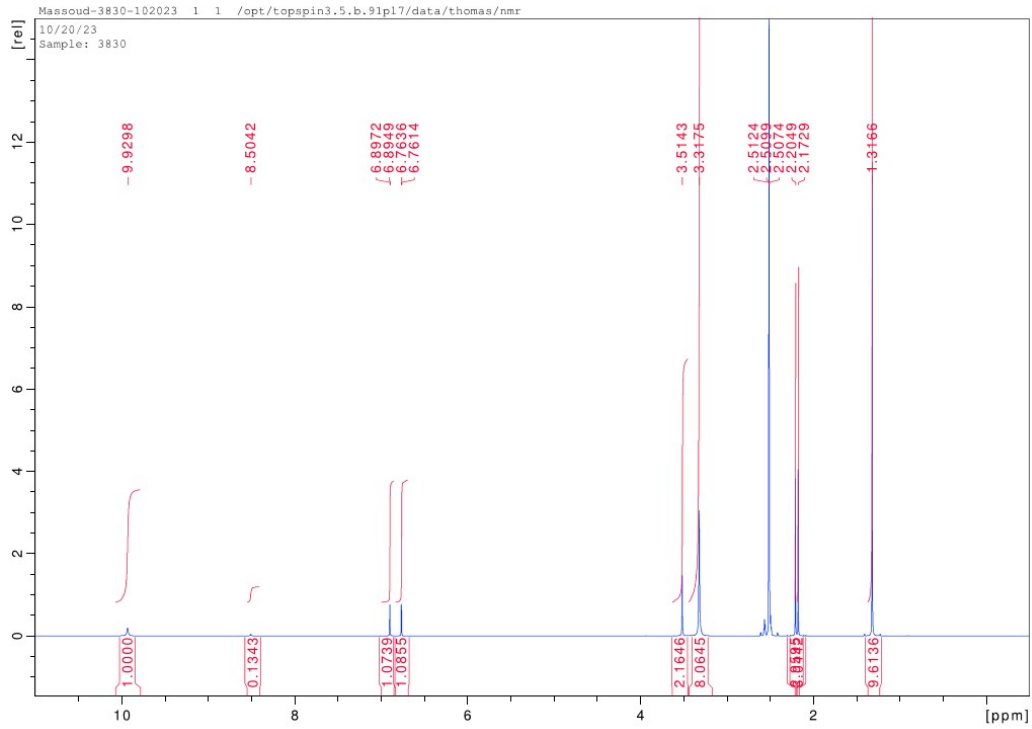


Fig. S2. ^1H NMR spectra of H_2L^3 in d_6 -DMSO.

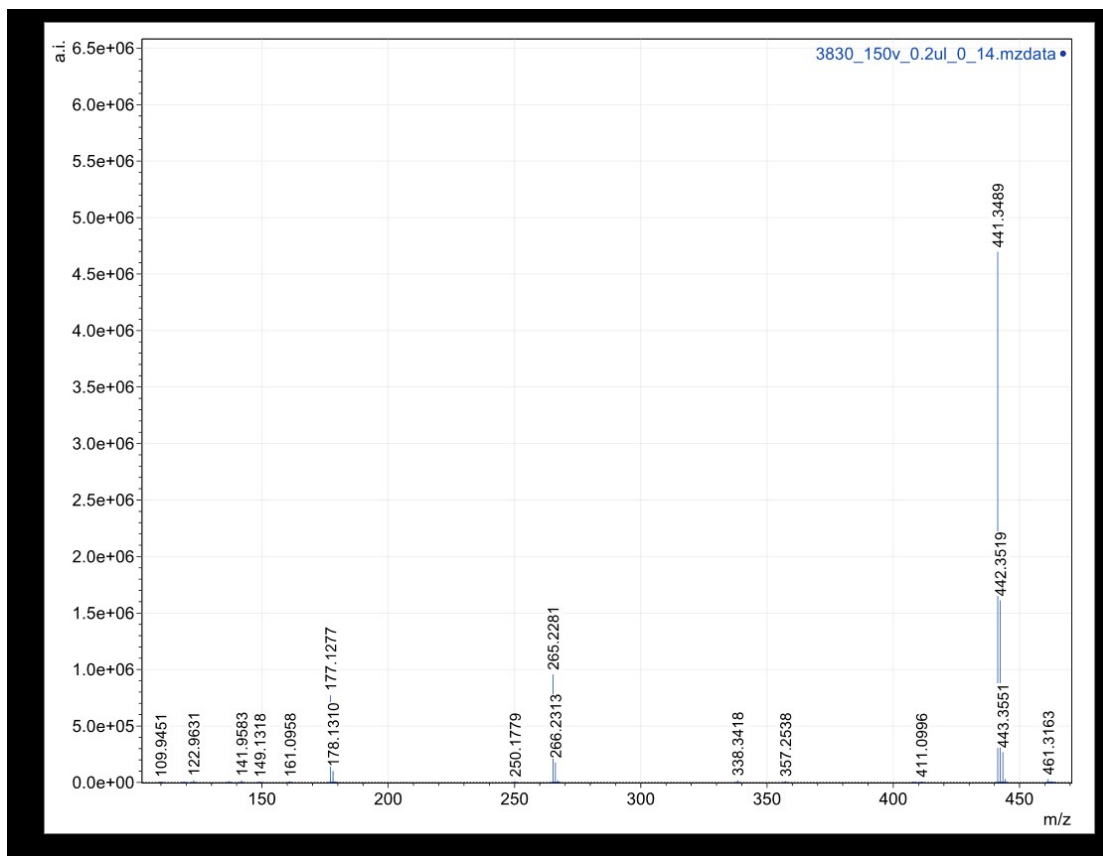
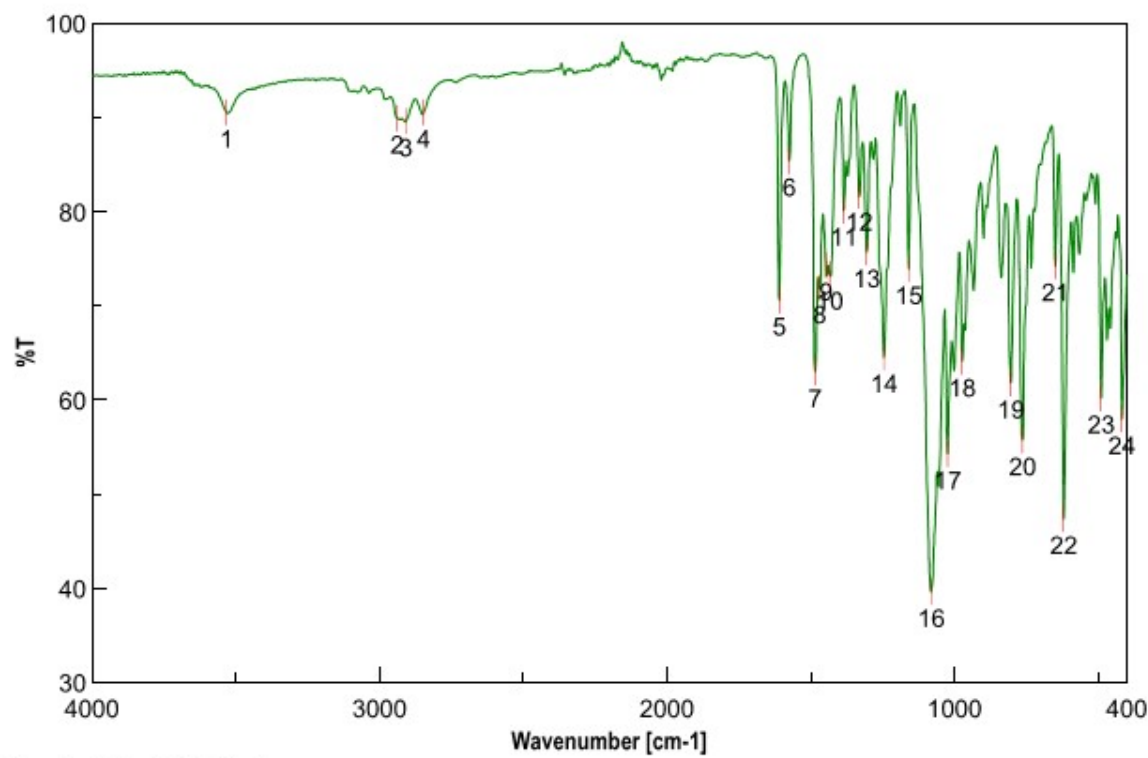


Fig. S3. ESI-MS of H_2L^3 in CH_3OH .

Peak Find - 3681.jws



[Result of Peak Picking]

No.	Position	Intensity	No.	Position	Intensity
1	3531.99	90	2	2938.98	90
3	2908.13	90	4	2846.42	90
5	1609.31	71	6	1574.59	85
7	1484.92	63	8	1469.49	72
9	1447.31	74	10	1433.82	73
11	1384.64	80	12	1331.61	82
13	1305.57	76	14	1244.83	64
15	1159.01	74	16	1080.91	40
17	1024.02	54	18	972.912	64
19	804.171	62	20	763.673	56
21	649.893	74	22	620.002	47
23	489.831	60	24	417.513	58

Fig. S4. IR spectrum of $[\text{Zn}_2(\text{L}^1)_2](\text{ClO}_4)_2$ (**1**)

Agilent Resolutions Pro

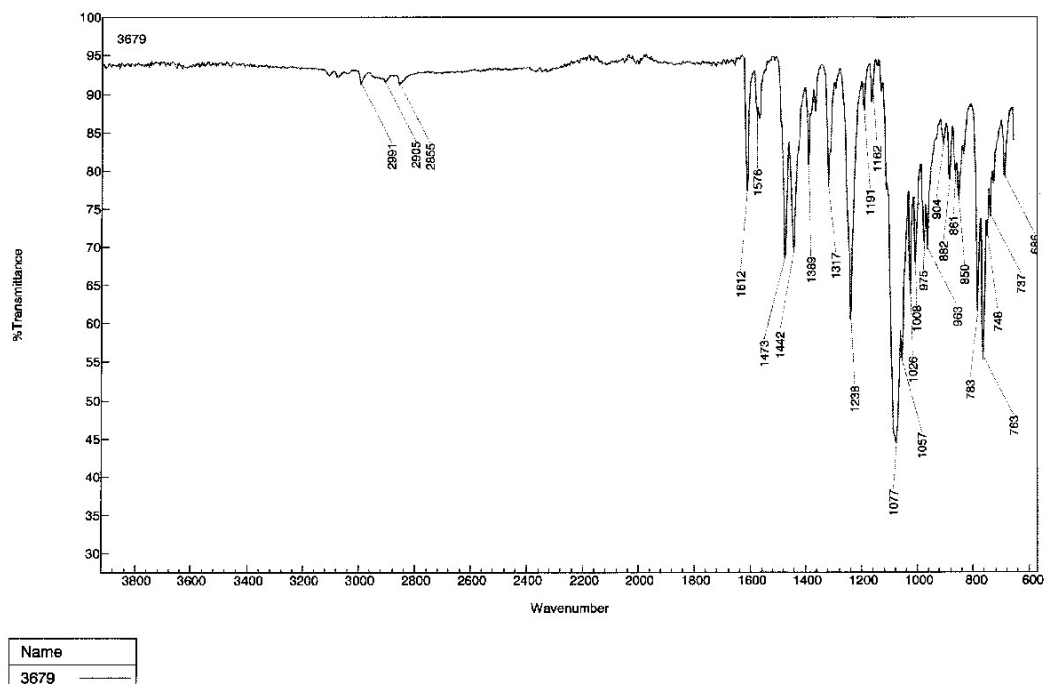
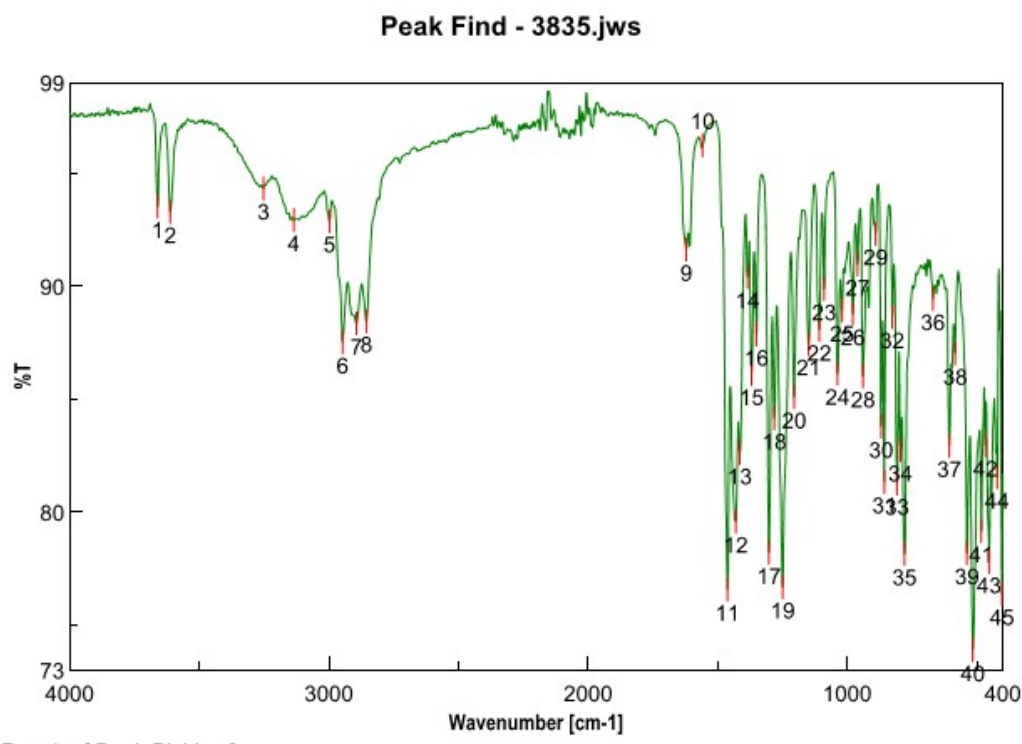


Fig. S5. IR spectrum of $[\text{Zn}_2(\text{L}^2)_2](\text{ClO}_4)_2$ (**2**)

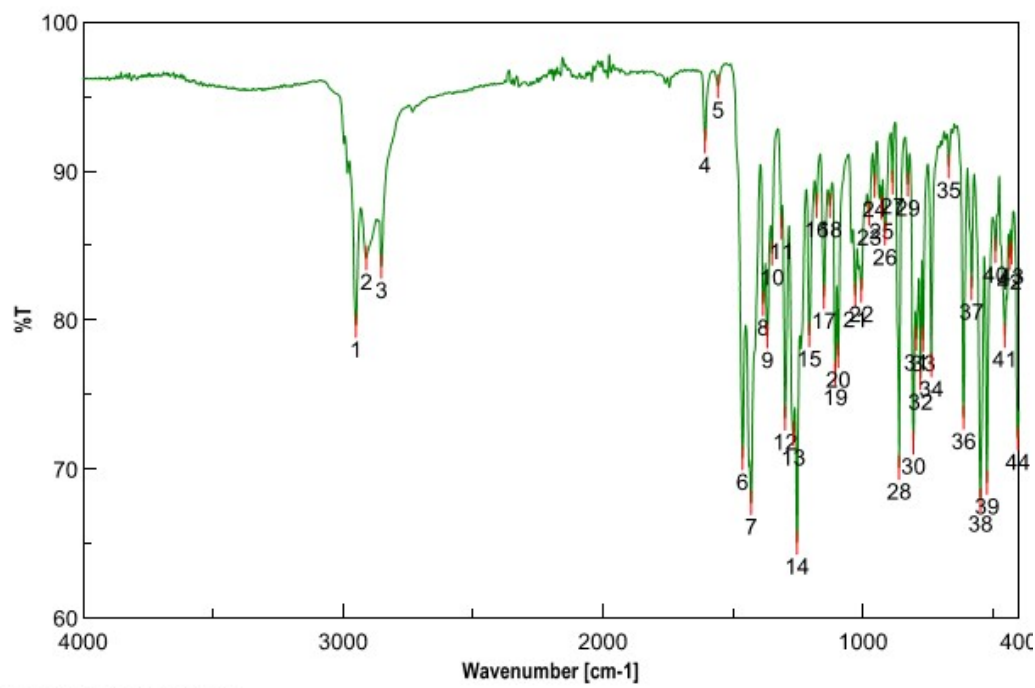


[Result of Peak Picking]

No.	Position	Intensity	No.	Position	Intensity
1	3660.23	94	2	3611.05	93
3	3252.36	94	4	3134.72	93
5	2997.8	93	6	2946.7	88
7	2893.66	88	8	2855.1	88
9	1620.88	92	10	1558.2	96
11	1461.78	77	12	1429.96	80
13	1414.53	83	14	1384.64	90
15	1369.21	86	16	1350.89	88
17	1301.72	78	18	1281.47	84
19	1249.65	77	20	1205.29	85
21	1149.37	87	22	1107.9	88
23	1089.58	90	24	1037.52	86
25	1020.16	89	26	978.697	89
27	960.377	91	28	939.163	86
29	890.952	92	30	868.774	84
31	857.204	81	32	826.348	89
33	808.028	81	34	794.528	83
35	779.101	78	36	669.178	89
37	606.503	83	38	584.325	87
39	538.042	78	40	515.865	74
41	483.081	79	42	467.653	83
43	452.225	78	44	421.37	82
45	403.05	76			

Fig. S6. IR spectrum of $[\text{Zn}(\text{L}^3)(\text{H}_2\text{O})] \cdot \text{CH}_3\text{OH}$ (**3**).

Peak Find - 3836.jws

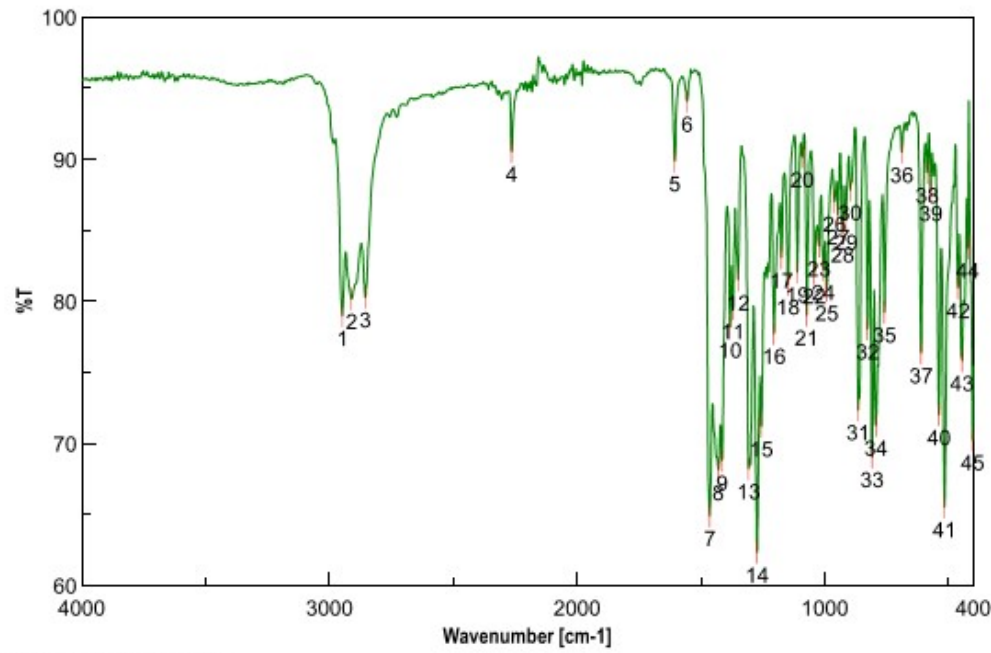


[Result of Peak Picking]

No.	Position	Intensity	No.	Position	Intensity
1	2950.55	80	2	2911.02	84
3	2852.2	84	4	1607.38	92
5	1557.24	96	6	1463.71	71
7	1429.96	68	8	1383.68	81
9	1367.28	79	10	1348.96	84
11	1313.29	86	12	1298.82	73
13	1267.97	72	14	1253.5	65
15	1206.26	79	16	1178.29	88
17	1149.37	82	18	1127.19	88
19	1105.98	76	20	1094.4	78
21	1028.84	82	22	1005.7	82
23	975.804	87	24	954.591	89
25	928.557	88	26	915.058	86
27	886.131	89	28	860.096	70
29	827.312	89	30	805.135	72
31	794.528	79	32	778.136	76
33	767.53	79	34	736.674	77
35	669.178	90	36	612.288	73
37	581.433	82	38	547.685	68
39	522.615	69	40	489.831	85
41	453.19	79	42	435.834	84
43	427.155	85	44	403.05	72

Fig. S7. IR spectrum of $[\text{Zn}(\text{L}^4)]$ (**4**).

Peak Find - 3827



[Result of Peak Picking]					
No.	Position	Intensity	No.	Position	Intensity
1	2947.66	79	2	2911.02	80
3	2855.1	80	4	2264.02	91
5	1606.41	90	6	1556.27	94
7	1464.67	65	8	1429.96	68
9	1415.49	69	10	1382.71	78
11	1371.14	79	12	1349.93	81
13	1307.5	68	14	1272.79	62
15	1256.4	71	16	1205.29	78
17	1174.44	83	18	1148.4	81
19	1110.8	82	20	1091.51	90
21	1073.19	79	22	1042.34	82
23	1024.02	84	24	1005.7	82
25	992.196	81	26	960.377	87
27	945.913	86	28	928.557	85
29	915.058	86	30	897.701	88
31	865.882	72	32	827.312	78
33	808.992	69	34	793.564	71
35	758.852	79	36	689.427	90
37	611.324	76	38	587.218	89
39	572.755	88	40	539.007	72
41	516.829	65	42	461.868	81
43	445.476	76	44	423.298	84
45	403.05	70			

Fig. S8. IR spectrum of [Zn(L⁵)] (**5**).

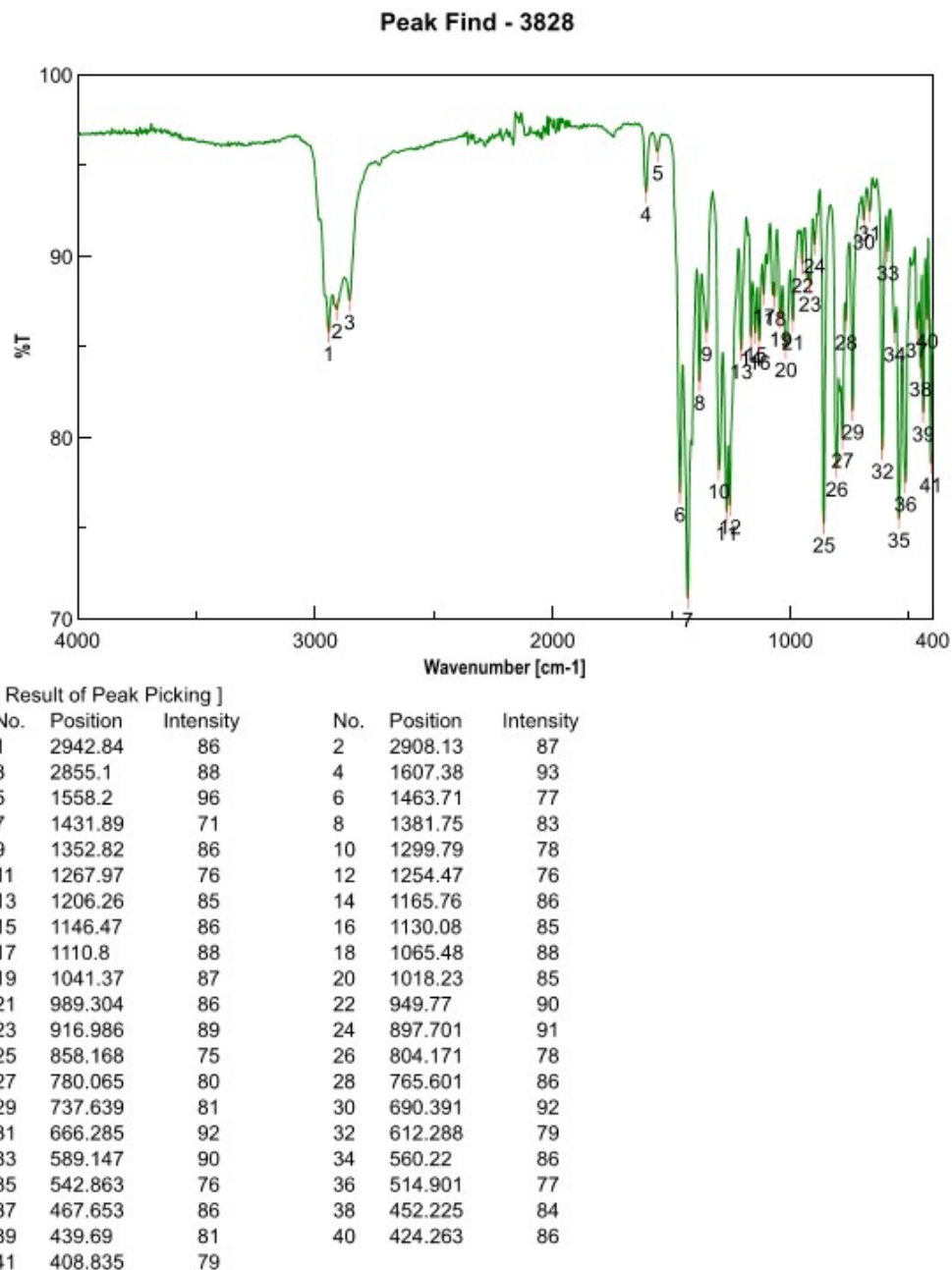


Fig. S9. IR spectrum of $[Zn(L^6)]$ (6).

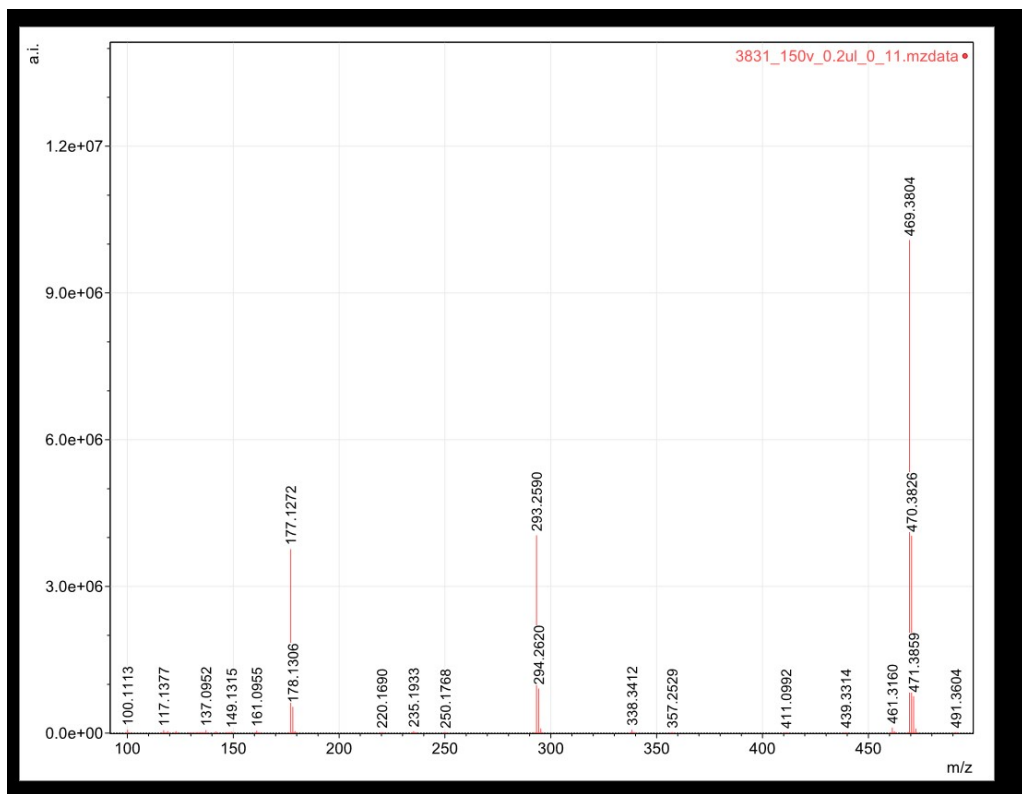


Fig. S10. ESI-MS of H_2L^4 in CH_3OH .

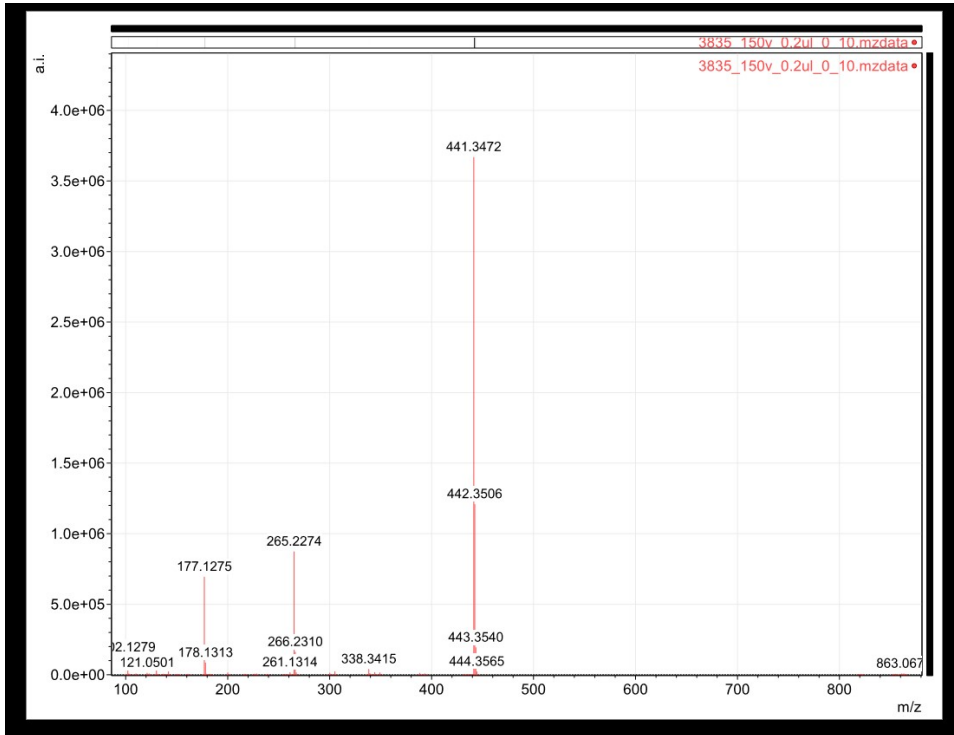


Fig. S11. ESI-MS of complex 3 in CH_3CN .

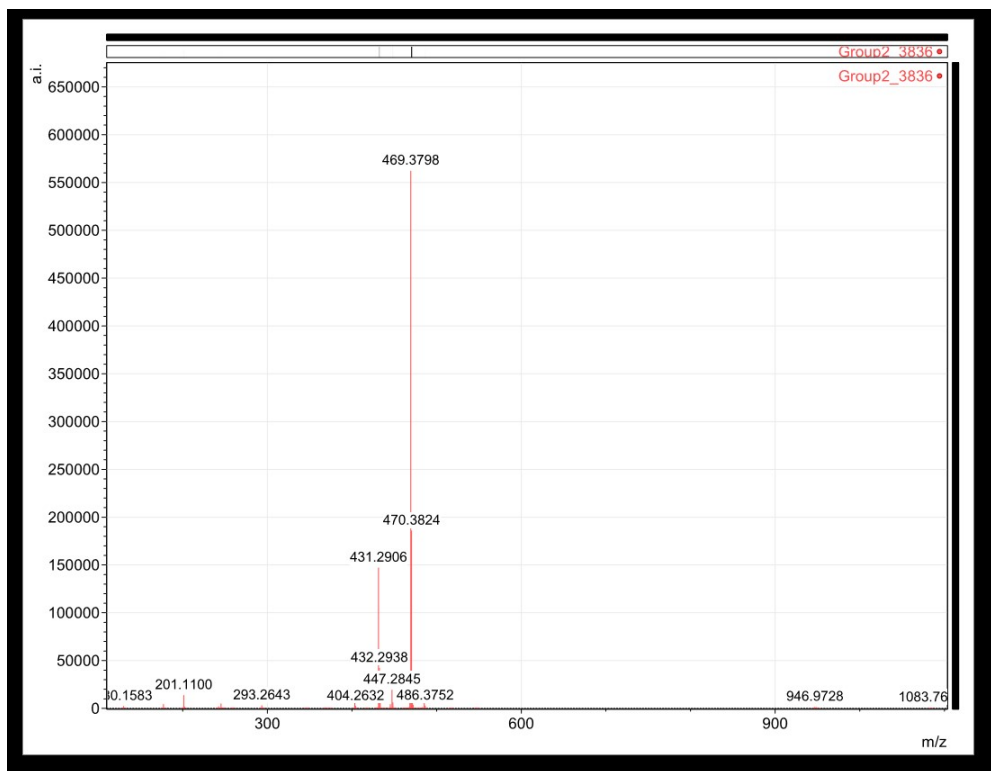


Fig. S12. ESI-MS of complex 4 in CH_3CN .

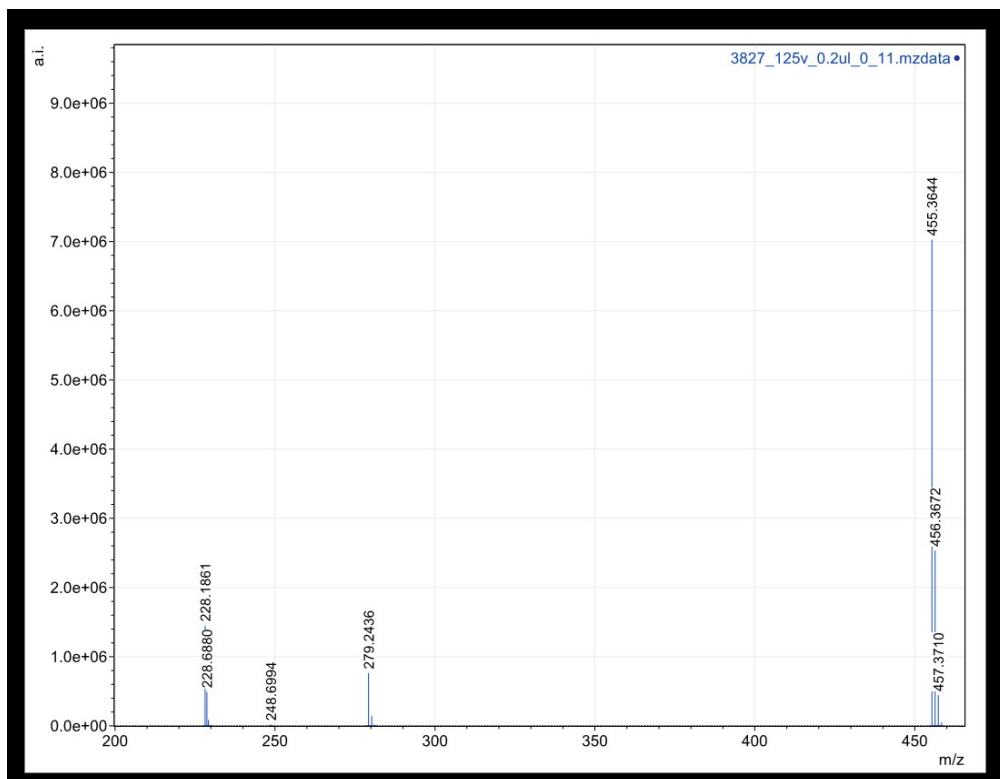


Fig. S13. ESI-MS of complex 5 in CH_3CN .

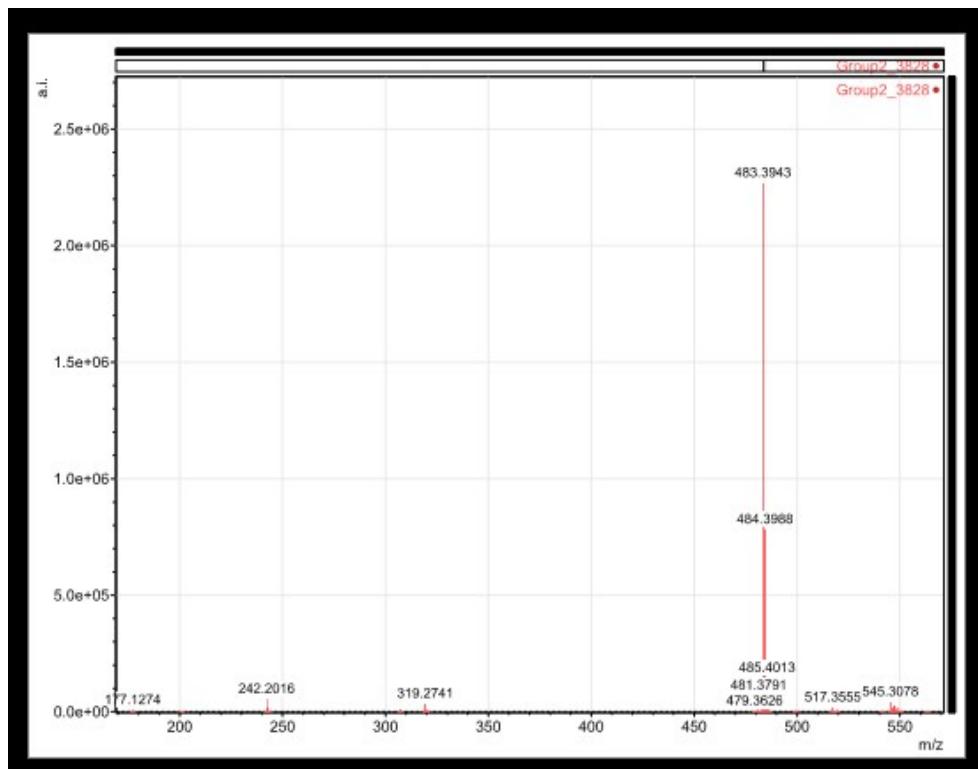


Fig. 14. ESI-MS of complex **6** in CH_3CN .

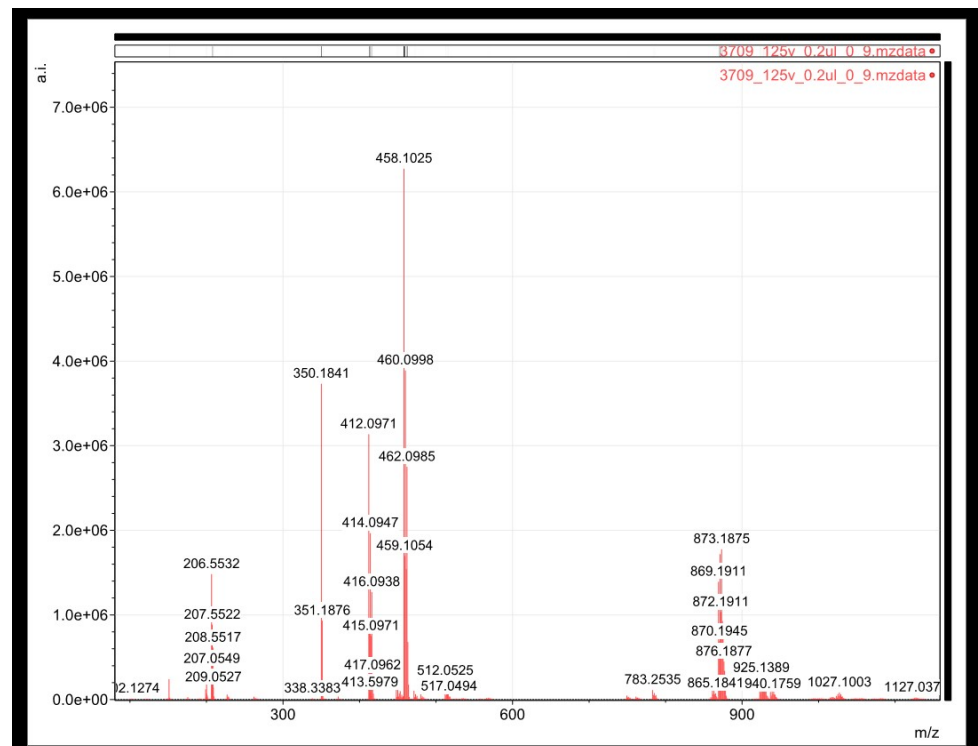


Fig. S15. ESI-MS of **1** in CH_3CN .

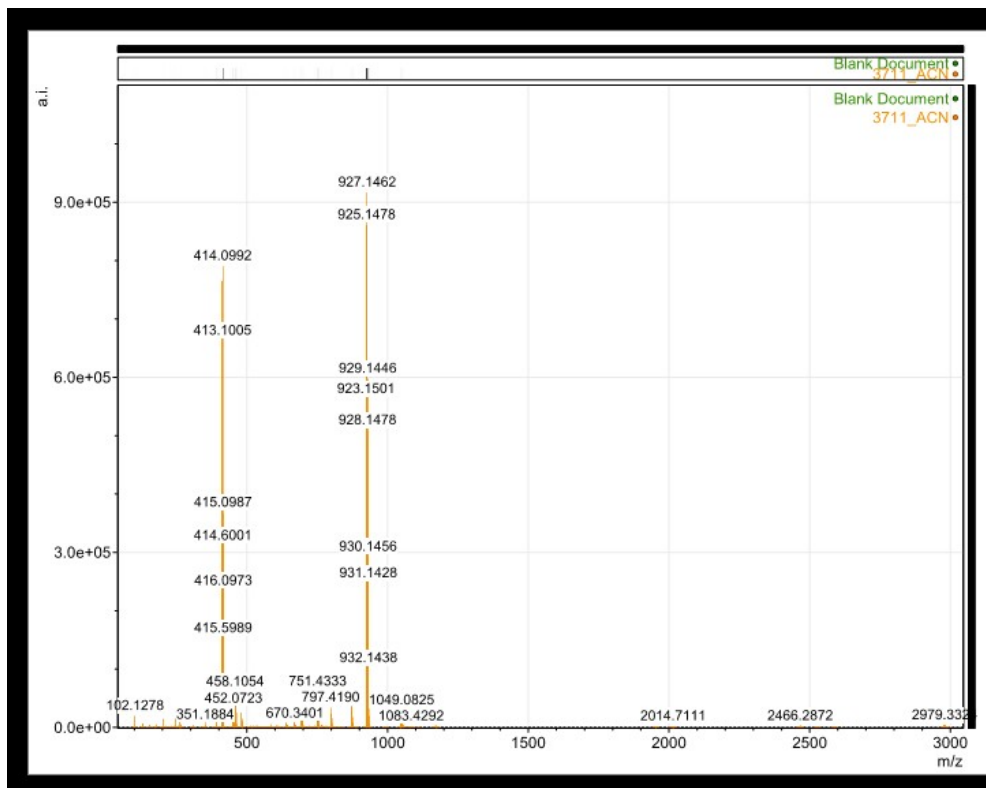


Fig. S16. ESI-MS of complex **2** in a CH₃CN/HCOOH (1:1) mixture.

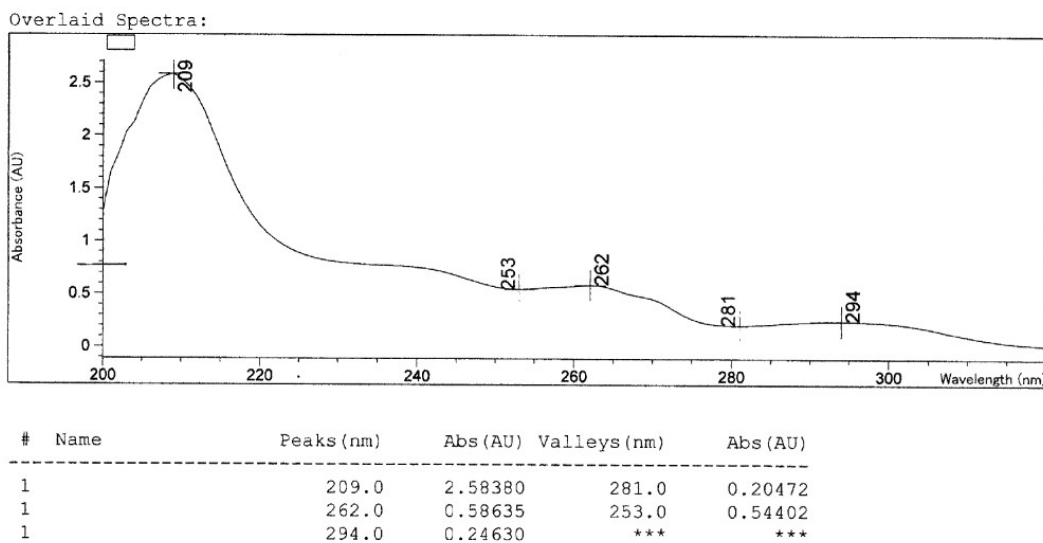


Fig. S17. UV spectrum of **1** (3.64×10^{-5} M) in MeOH.

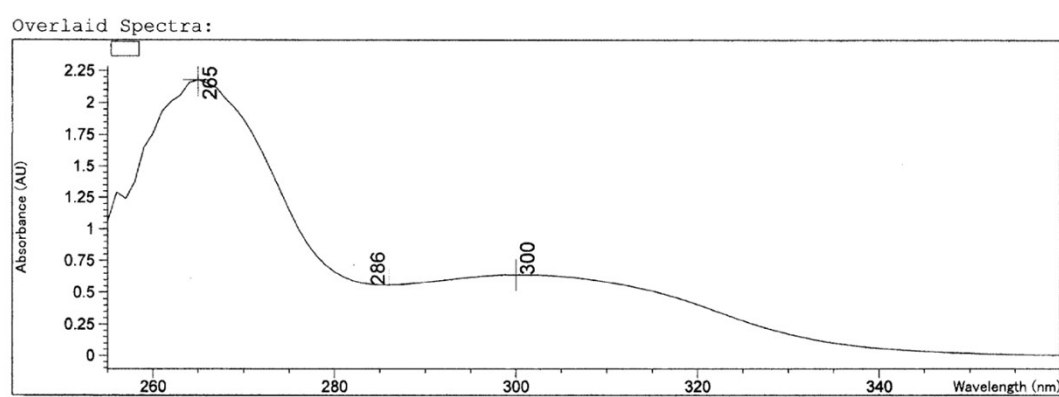
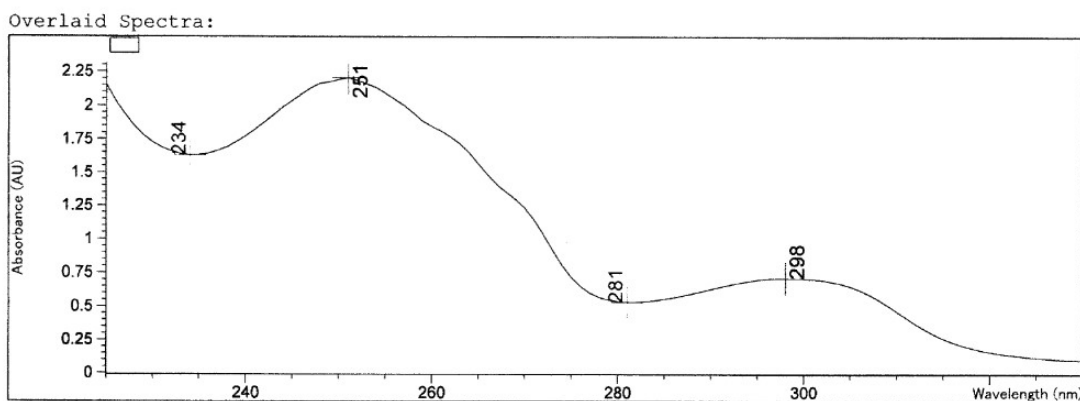


Fig. S18. UV spectrum of **2** in CH_3CN ($8.994 \times 10^{-5} \text{ M}$) (top) and in DMSO ($1.04 \times 10^{-4} \text{ M}$) (bottom).

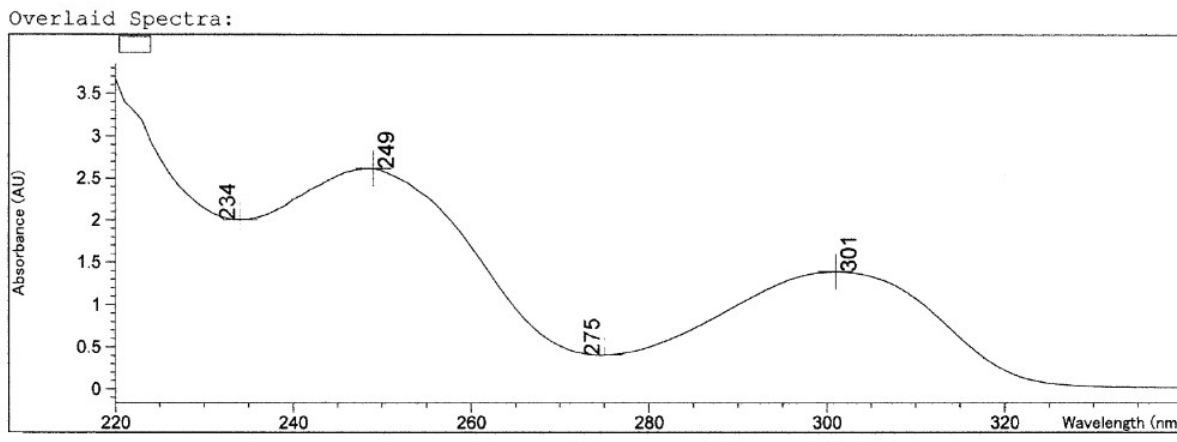


Fig. S19. UV spectrum of **4** in CH_3CN (2.067×10^{-4} M).

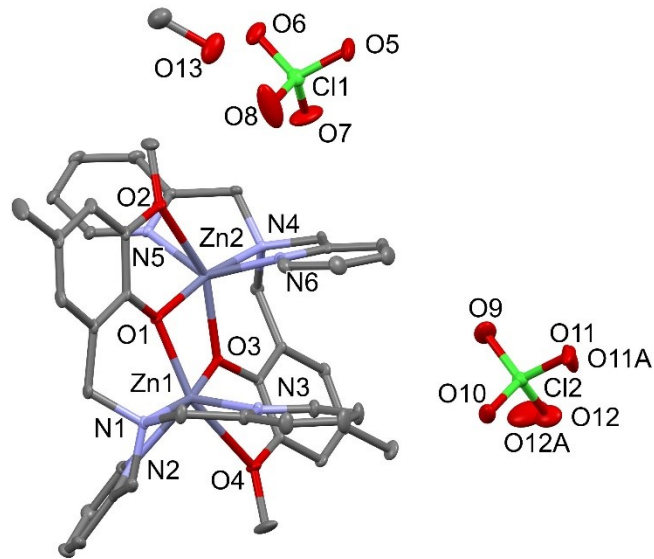


Fig. S20: ORTEP view of **1** showing also disordered parts of the complex.

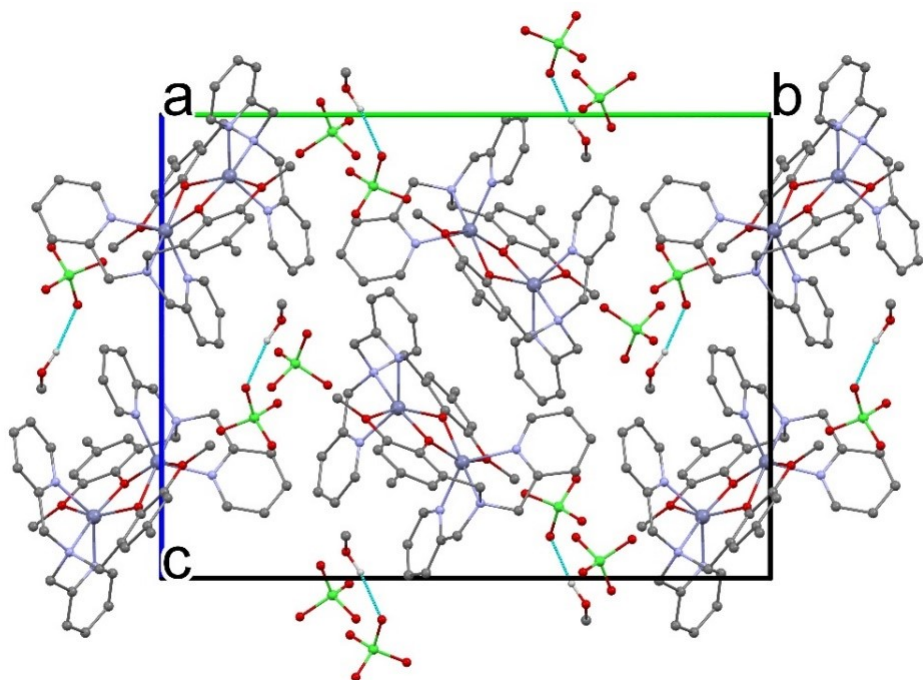


Fig. S21. Packing plot of 1.

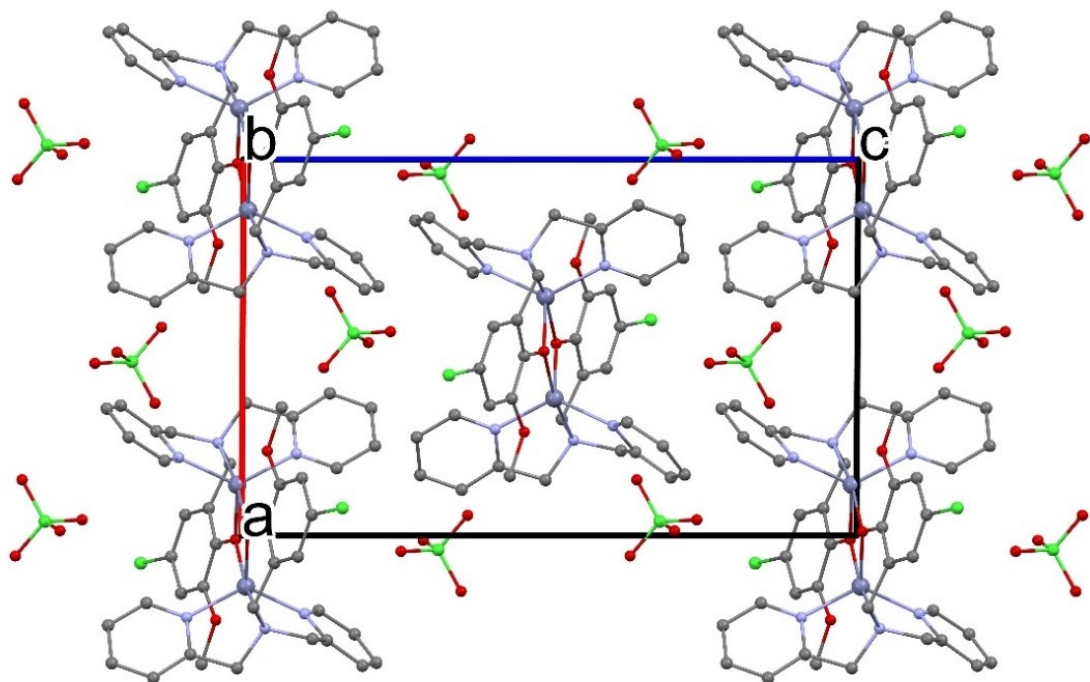


Fig. S22. Packing plot of 2.

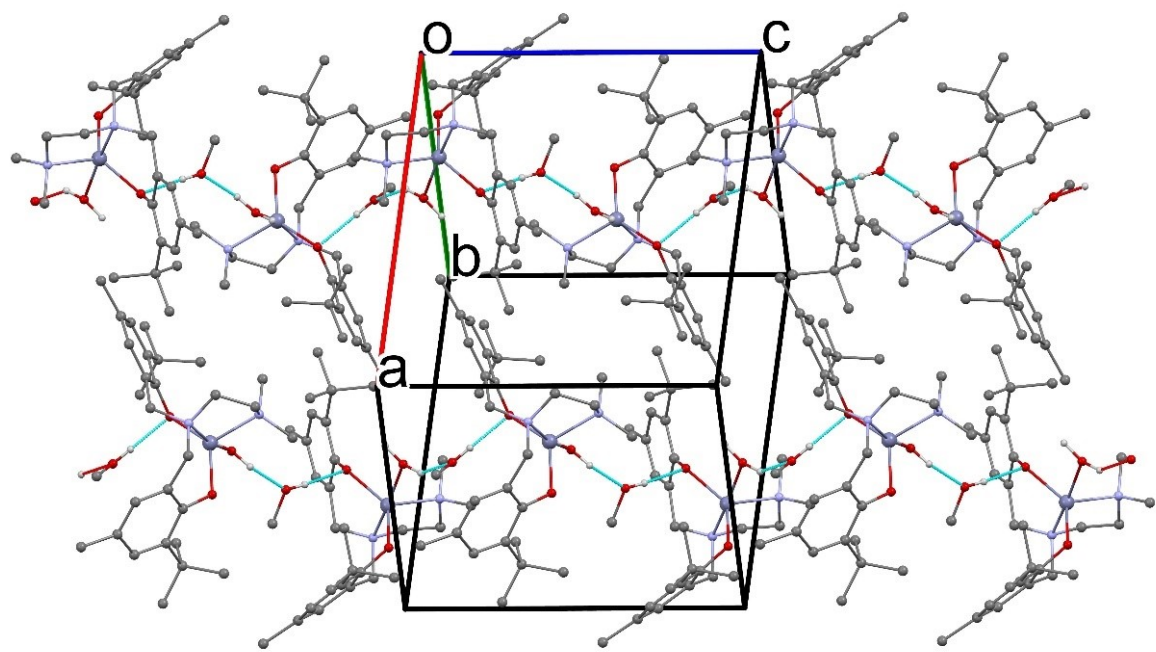


Fig. S23. Packing plot of 3.

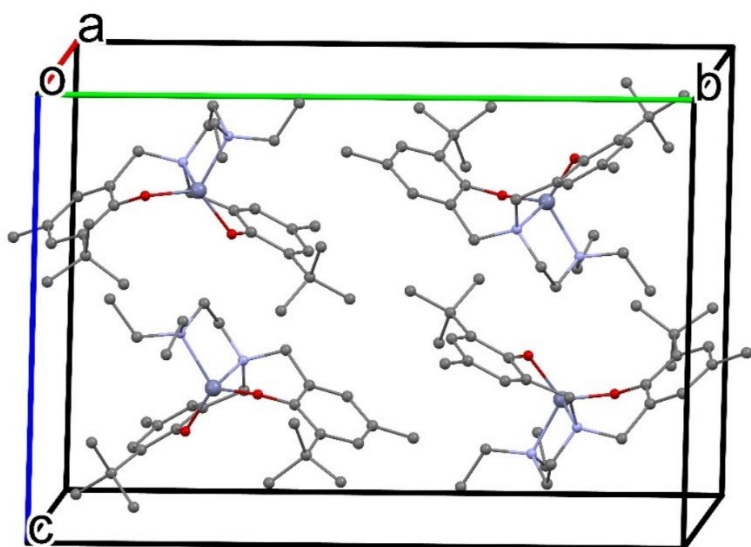


Fig. S24. Packing plot of 4.

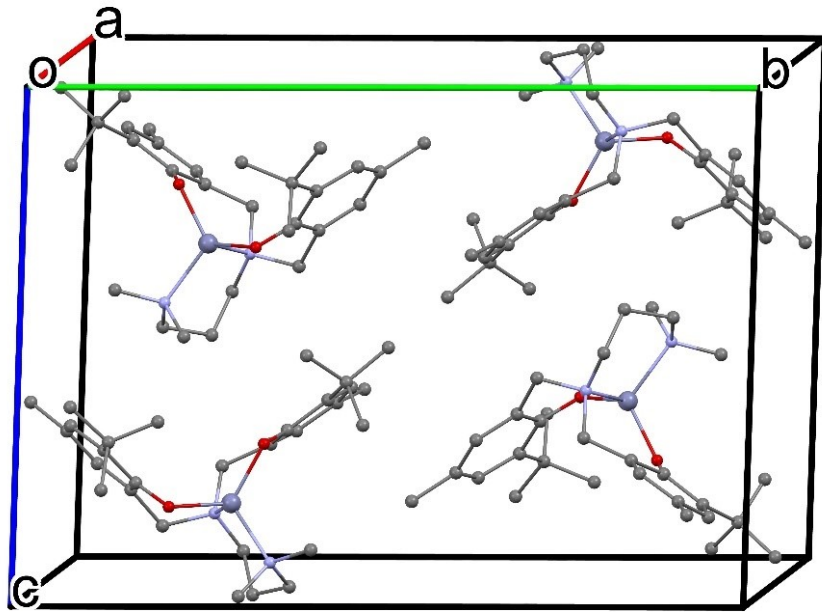


Fig. S25. Packing plot of **5**.

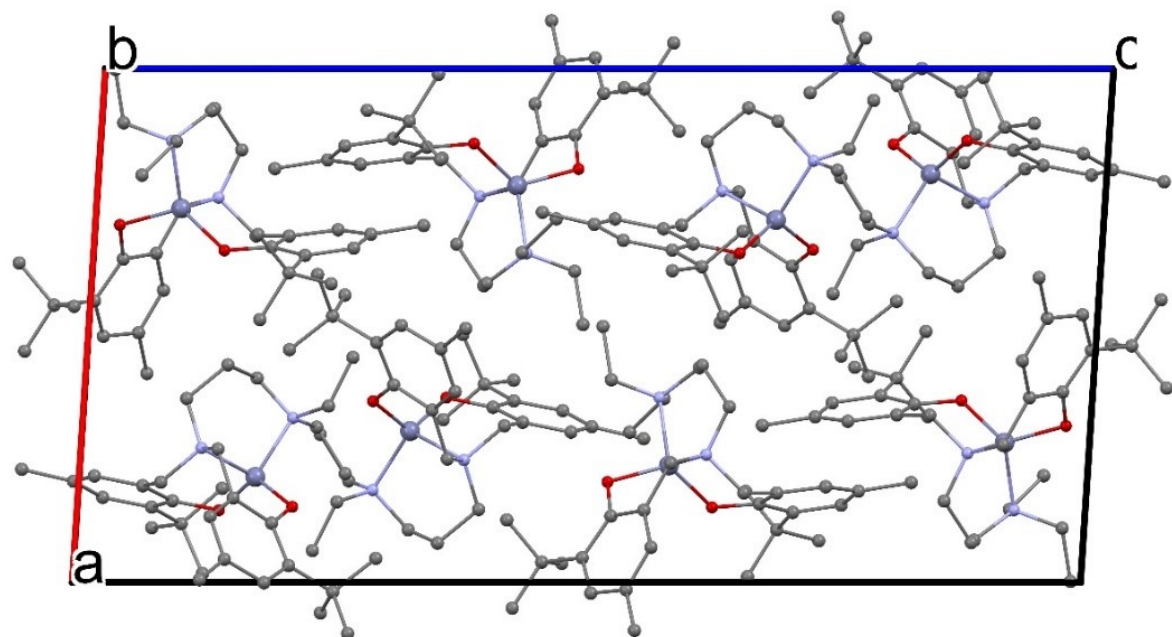


Fig. S26. Packing plot of **6**.

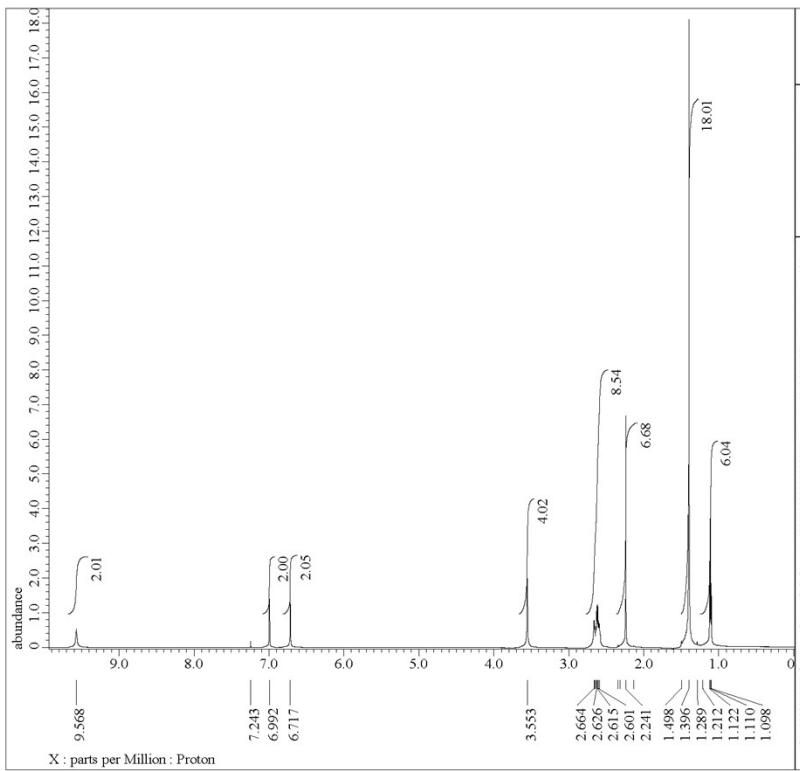


Fig. S27. ^1H NMR spectrum of free H_2L^4 measured in CDCl_3 .

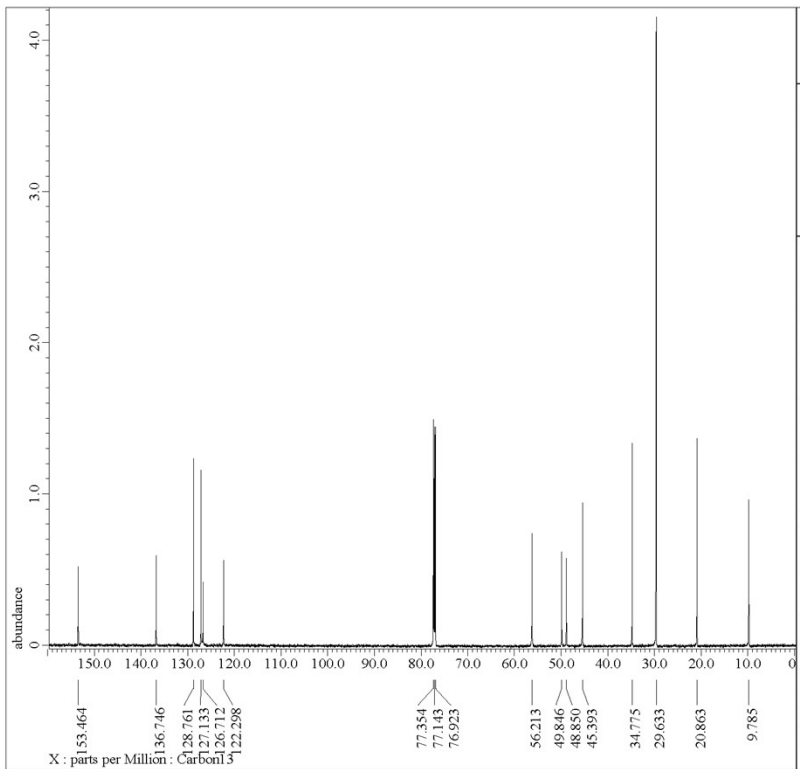


Fig. S28. ^{13}C NMR spectrum of free H_2L^4 measured in CDCl_3 .

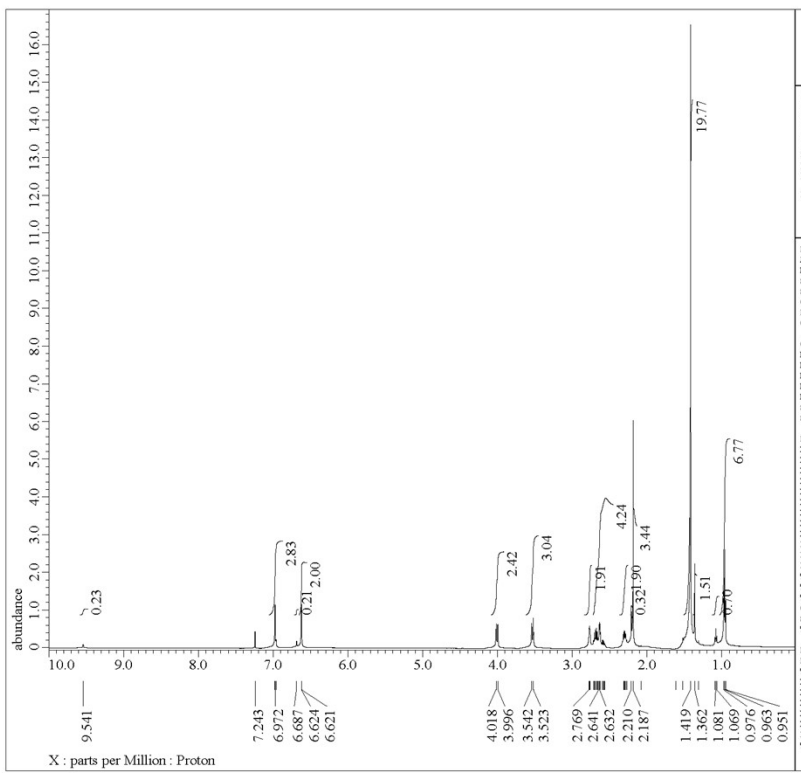


Fig. S29. ^1H NMR spectrum of $[\text{Zn}(\text{L}^4)]$ (**4**) measured in CDCl_3 immediately after the sample dissolution.

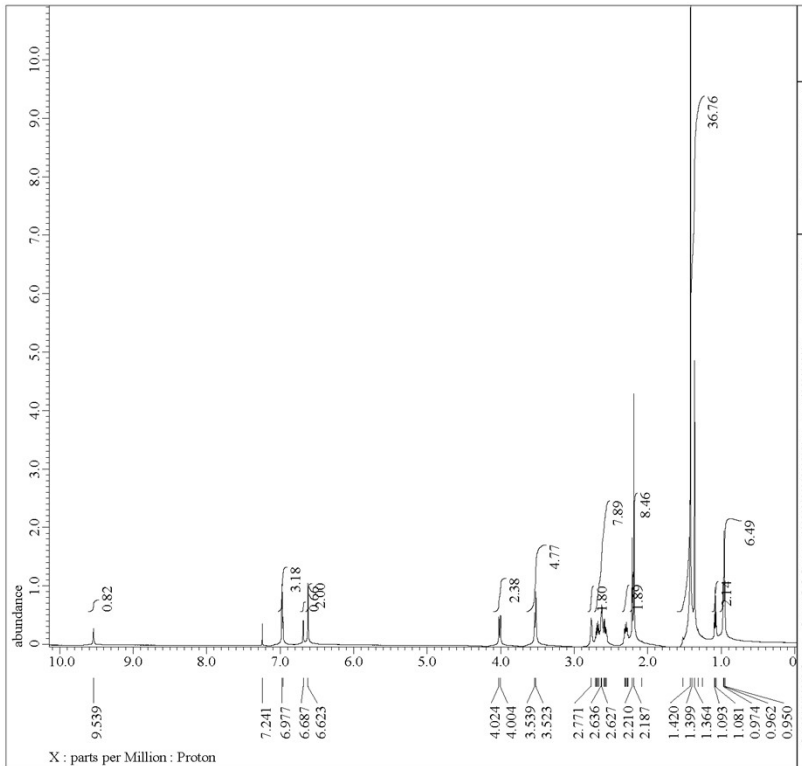


Fig. S30. ^1H NMR spectrum of $[\text{Zn}(\text{L}^4)]$ (**4**) measured in CDCl_3 22 h after the sample dissolution.

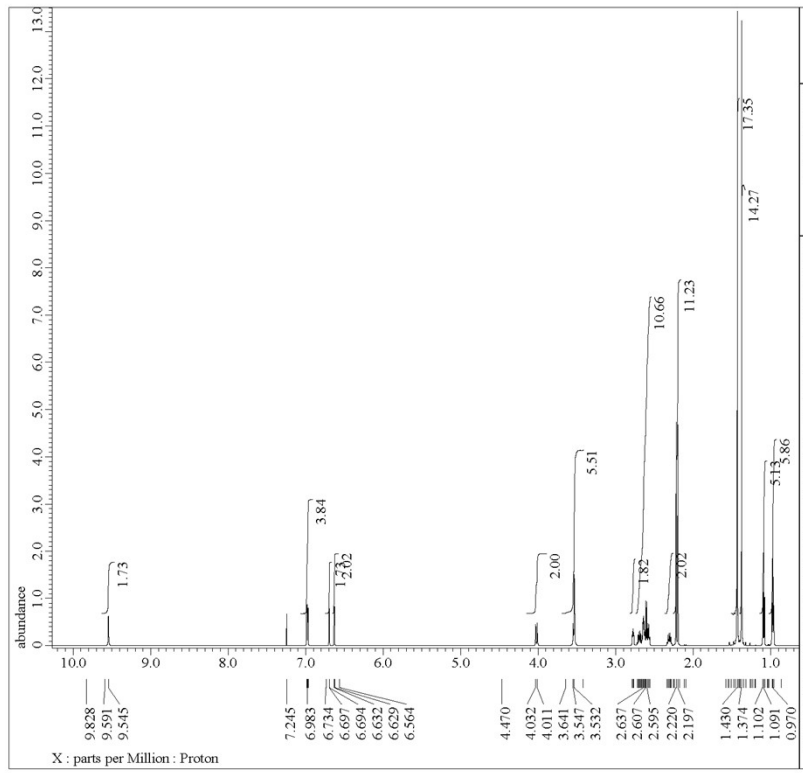


Fig. S31. ^1H NMR spectrum of $[\text{Zn}(\text{L}^4)]$ (4) measured in CDCl_3 6 days after the sample dissolution.

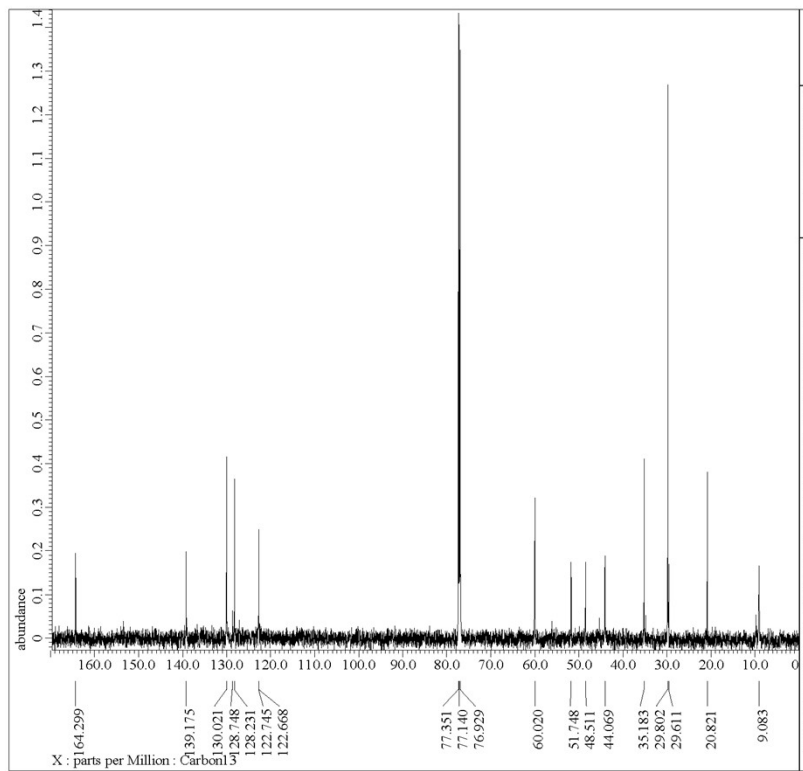


Fig. S32. ^{13}C NMR spectrum of $[\text{Zn}(\text{L}^4)]$ (**4**) measured in CDCl_3 immediately after the sample dissolution.

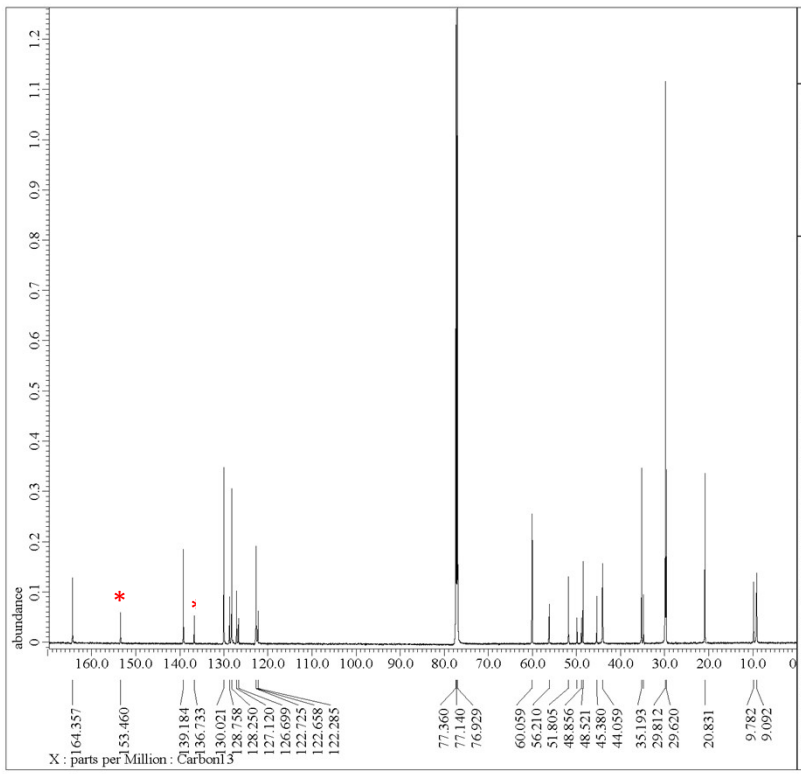


Fig. S33. ^{13}C NMR spectrum of $[\text{Zn}(\text{L}^4)]$ (4) measured in CDCl_3 22 h after the sample dissolution. *The selected signals belonging to the free H_2L^4 ligand.

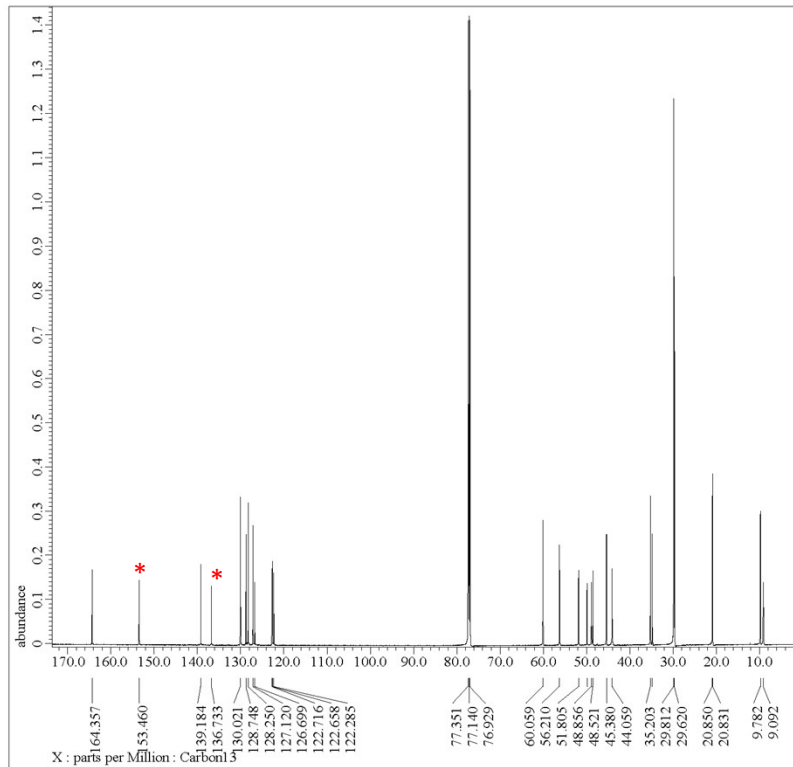


Fig. S34. ^{13}C NMR spectrum of $[\text{Zn}(\text{L}^4)]$ (4) measured in CDCl_3 6 days after the sample dissolution. *The selected signals belonging to the free H_2L^4 ligand.

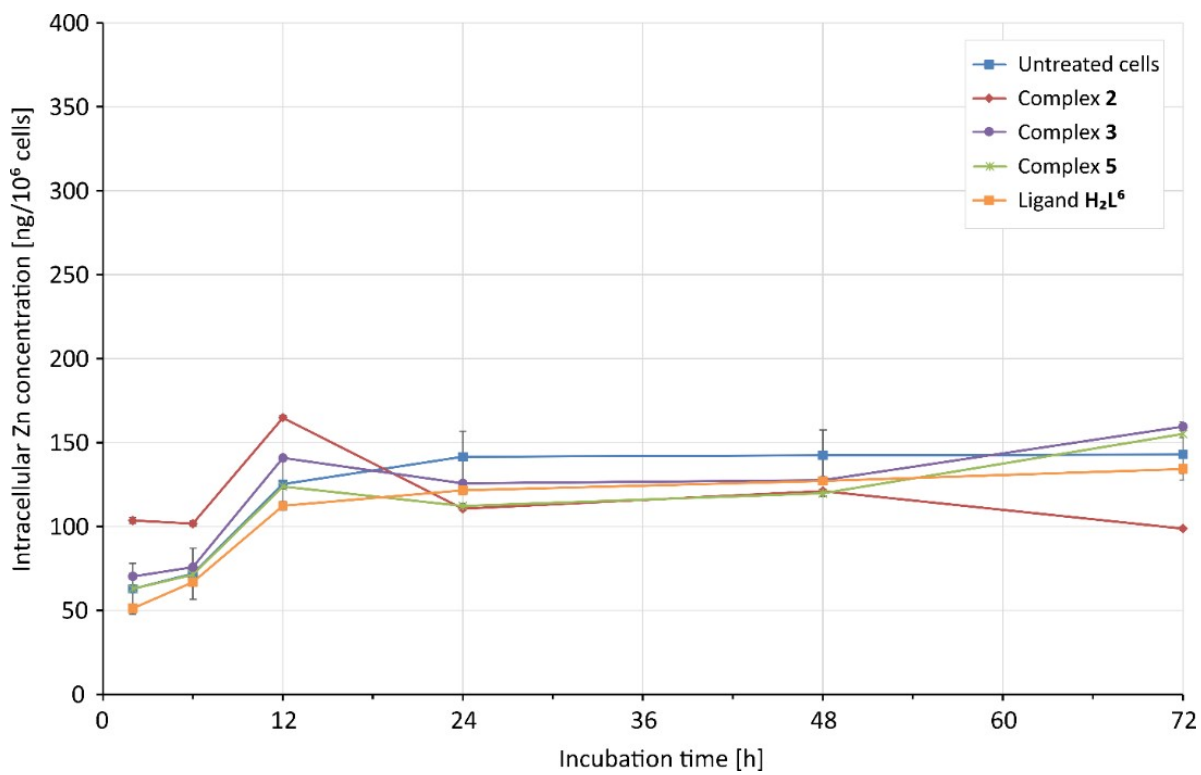


Fig. S35. The effect of complexes **2**, **3**, and **5**, and ligand **H₂L⁶** on intracellular levels of zinc in A2780 cells incubated with half-toxic concentrations of the compounds for 2, 6, 12, 24, 48, and 72 h. The determined values are averages from three parallel determinations \pm standard deviation.